J Fluoresc (2011) 21:1607–1615
DOI 10.1007/s10895-011-0849-8

ORIGINAL PAPER

Directly Oxidized Chemiluminescence of 2-Substituted-4,5-di (2-Furyl)-1*H* -Imidazole by Acidic Potassium Permanganate and its Analytical Application for Determination of Albumin

Jing Kang · Yumin Zhang · Zhongxiu Huang · Lu Han · Jieli Tang · Shuaijun Wang · Yihua Zhang

Received: 22 November 2010 / Accepted: 12 January 2011 / Published online: 28 January 2011

Abstract In the paper, 2,4,5-tri(2-furyl)-1*H*-imidazole (TFI) and 2-phenyl-4,5-di(2-furyl)-1*H*-imidazole (PDFI), were chosen to investigate chemiluminescence (CL) properties of 2-substituted-4,5-di(2-furyl)-1*H*-imidazoles. The directly oxidized CL of analytes by potassium permanganate ($KMnO_4$) was in detail studied. The $KMnO_4$ could directly oxidize TFI/PDFI to produce strong CL emission in acidic solution. The effects of experimental conditions were investigated. Under the optimal conditions, the effect of albumin on the TFI/PDFI-$KMnO_4$ system was investigated. It was found that the addition of albumin into the system could induce enhancement of CL signal, and the enhanced CL intensity is linearly related to the logarithm of concentration of albumin. Based on this study, a novel CL method has been developed for the determination of albumin with high sensitivity and good selectivity. The method was applied to the determination of albumin in human serum samples, and the results were in agreement with those obtained by the bromcresol green (BCG) method. The relative errors for the analytical results were from −5.8% to 4.2%. These new phenomena would further enable people to exploit more CL analytical application of the heterocyclic imidazole derivatives.

Keywords Chemiluminescence · 2,4,5-tri(2-furyl)-1*H*-imidazole · 2-phenyl-4,5-di(2-furyl)-1*H*-imidazole · Potassium permanganate · Albumin

J. Kang · Y. Zhang · L. Han · J. Tang · S. Wang · Y. Zhang (✉)
College of Chemistry, Jilin University,
Changchun 130012, People's Republic of China
e-mail: yihuazh47@yahoo.com.cn

Z. Huang
Qianwei Hospital, Jilin University,
Changchun 130012, People's Republic of China

Introduction

Over the years, heterocyclic imidazole derivatives have attracted considerable attention because of their unique optical properties [1–3]. These compounds play a very important role in chemistry as mediators for synthetic reactions, primarily as a means for preparing functionalized materials [4]. Imidazole nucleus forms the main structure of some well-known components of human organisms, i.e. the amino acid histidine, vitamin B_{12}, a component of DNA base structure, purines, histamine and biotin. It is also present in structures of many natural or synthetic drug molecules, i.e. azomycin, cimetidine and metronidazole [5]. Phenylimidazoles have been studied because of their important laser properties [6, 7]. Further substitution by phenyl groups results in other significant optical properties. An important imidazole derivative is lophine (2,4,5-triphenylimidazole). Recently, a number of lophine derivatives were synthesized based on lophine skeleton substituted at the *ortho*-, *meta*- and *para*-substituted in the 2-phenyl ring and *para*-substituted in the 4- and 5-aryl rings according to slightly modified procedure of the Debus method [8–13]. A variety of lophine analogues having 2-pyridyl or 2-furyl group at both 4- and 5-positions of heterocyclic imidazole derivatives have been reported [12, 13]. Among the derivatives, compounds carrying a 2-furyl group showed strong photoluminescence (PL) intensities, while those having a 2-pyridyl group gave very weak intensities [4]. Hitherto, many heterocyclic imidazole derivatives have been synthesized and studied with regard to their ultraviolet (UV), PL and chemiluminescence (CL) properties [11, 12].

The CL can be defined as emission of light (ultraviolet, visible or infrared) from a molecule or atom in an electronically excited state produced by a chemical reaction at ordinary temperature without any associated generation

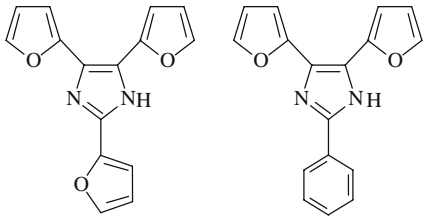

Fig. 1 Molecular structures of TFI and PDFI

of heat. The CL has attracted a great deal of attention as an interesting and useful detection method in analytical chemistry [14–17]. The CL detection has a number of advantages: (i) high detection sensitivity, (ii) wide linear range of signal response, (iii) inexpensive reagent and apparatus, (iv) easy and rapid measurement. Lophine is a well-known potential CL compound synthesized by Radziszewski (1877). It has been used for analysis of some metal ions [18–21] and chlorinated compounds [20]. The study of CL of heterocyclic imidazole derivatives was limited to system of H_2O_2 as oxidant for the CL reaction [4]. In this paper, the direct oxidation of 2-substituted-4,5-di(2-furyl)-*1H*-imidazoles by acidic potassium permanganate ($KMnO_4$) was applied to producing CL signals.

$KMnO_4$, an important oxidant in many organic and inorganic redox reactions, involves the Mn(VII) entity, which is renowned for its versatility. The $KMnO_4$ oxidation process is eco-friendly and has gained importance in green chemistry. Chemical oxidation is full of illustrations of the use of many uni-atomic metallic ions as oxidants, e.g., Ag (I), Fe(III), Ce(IV), Cr(VI), Mn(VII), etc., and some large biological oxidants like flavin adenine dinucleotide (FAD), nicotinamide adenine dinucleotide phosphate (NADP), etc. $KMnO_4$, however, in various homogeneous and heterogeneous media, as well as on solid supports and in solvent free conditions, provides excellent results when used in a large number of oxidation processes. The $KMnO_4$ as a versatile oxidizing agent has been used to generate CL in many different medium (such as H_2SO_4, HCl, H_3PO_4, $NaHCO_3$ and NaOH) [22–24]. In 1920, Grinberg was the first to report the use of acidified $KMnO_4$ as a reagent for CL, as he investigated the oxidation of pyrogallol, also in the presence of hydrogen peroxide. Between 1936 and 1939, Audubert reported the oxidation of glucose by $KMnO_4$ to generate CL but did not specify whether the reaction was conducted under acidic or alkaline conditions. Over 40 years later, Mizuno et al. observed, using photon counting, what they described as extra-weak CL from the well-known oxidation of oxalic acid by $KMnO_4$ [22]. The acidic solutions of $KMnO_4$ have been extensively studied due to generating CL during the oxidation of both organic compounds and inorganic species [25–27]. Because of its importance as an analytical reagent, significant attention has also been given to elucidate the mechanism of the reaction with organic or inorganic substrates [28, 29].

In this paper, two 2-substituted-4,5-di(2-furyl)-*1H*-imidazoles, 2,4,5-tri(2-furyl)-1*H*-imidazole (TFI) and 2-phenyl-4,5-di(2-furyl)-1*H*-imidazole (PDFI), were synthesized according to the reported methods [30, 31] and their molecular structures are shown in Fig. 1. The $KMnO_4$ could directly oxidize TFI and PDFI to produce strong CL emission in acidic conditions. The effects of experimental

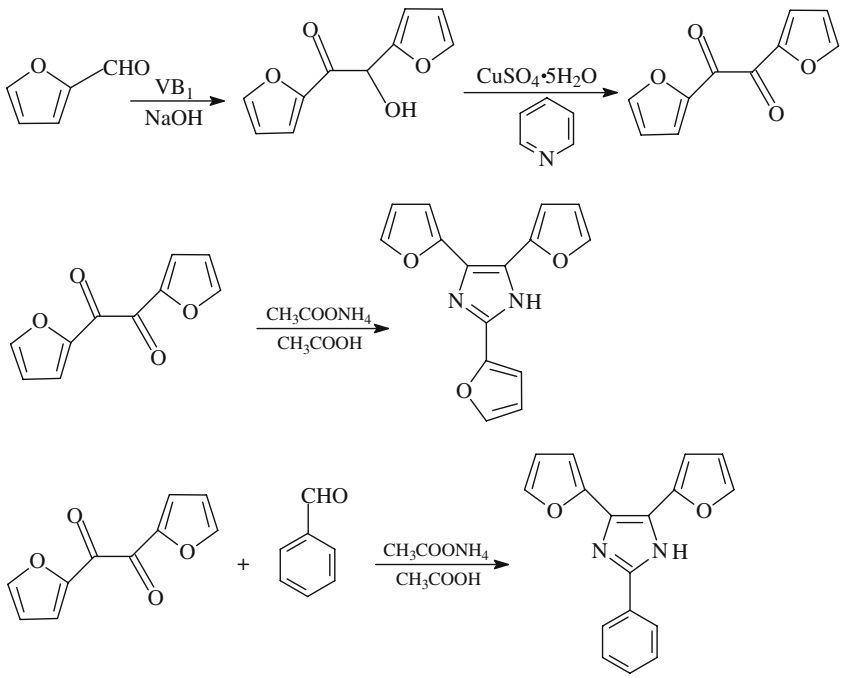

Fig. 2 Synthesis of TFI and PDFI

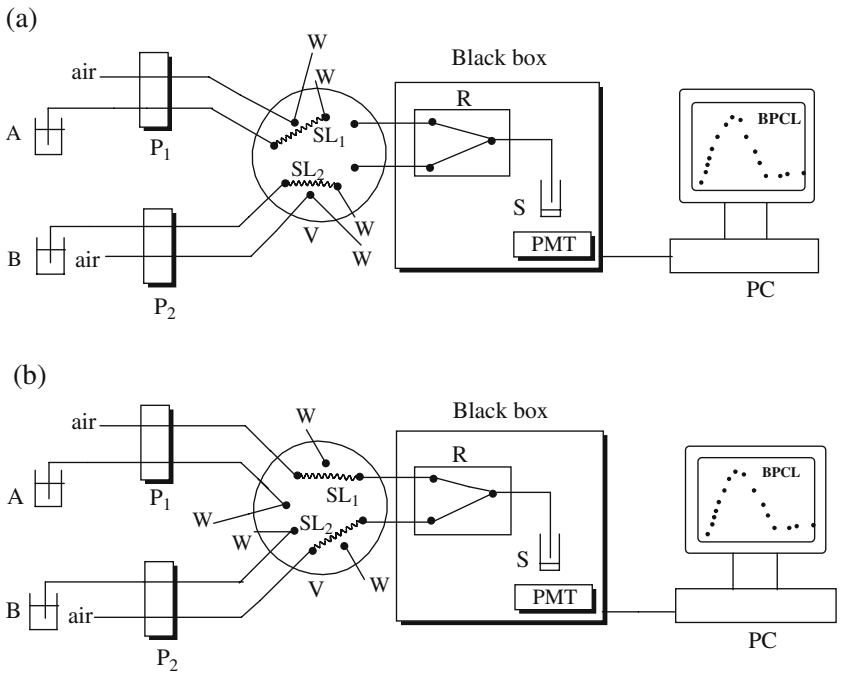

Fig. 3 Schematic diagram of the steady-injection CL system. A: $KMnO_4$ solution; B: HCl solution; P_1, P_2: peristaltic pump; SL: sample loop; V: eight-way valve; R: chemifold; S: sample cell; PMT: photomultiplier tube; PC: computer; W: waste. **a** Loading position. **b** Injection position

conditions were investigated. Under the optimal conditions, the experiments on the effect of albumin on the TFI/PDFI-$KMnO_4$ CL system was carried out and the result indicated that albumin could effectively enhance the CL signal of this reaction. The enhanced CL intensity is linearly related to the logarithm of concentration of albumin in the certain concentration range. The method was applied to the determination of albumin in human serum samples and the obtained results were satisfactory.

Experimental

Reagents and Chemicals

All the reagents were of analytical reagent grade and all solutions were prepared with ultra-pure water. Ammonium acetate, acetic acid, ethyl acetate, methanol, ammonium sulfate solution, $CuSO_4 \cdot 5H_2O$, $MgSO_4$, NaOH, $KMnO_4$, H_2SO_4, HCl, HNO_3 and H_3PO_4 were purchased from Beijing Chemical Plant in China. Furfural, petroleum ether and benzaldehyde were purchased from Tianjin Guangfu Fine Chemical Research Institute in China. Bovine serum albumin (BSA) and human serum albumin (HSA) were purchased from Sigma.

Synthesis of TFI and PDFI

The synthesis of TFI and PDFI is shown in Fig. 2. First, furil was synthesized from furfural by benzoic condensation and oxidation. TFI was synthesized according to the literature [30]. A mixture of 1 g furil (5.26 mmol) and 4.05 g ammonium acetate (52.6 mmol) in 20 mL acetic acid was heated and refluxed. After completion of the reaction,

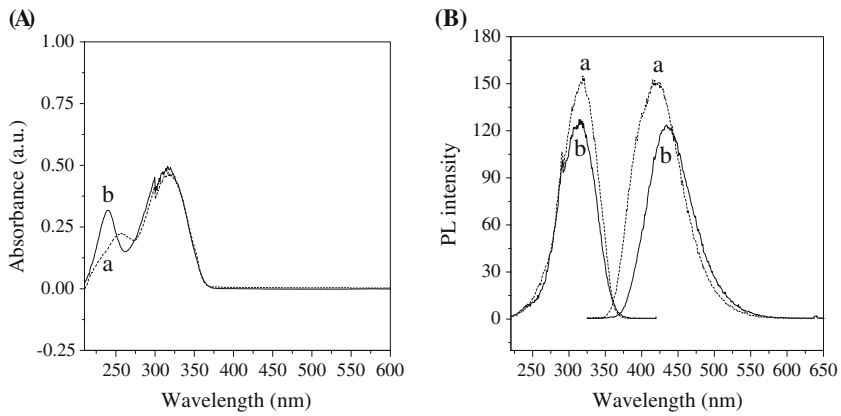

Fig. 4 Absorption spectra (**A**) and PL spectra (**B**) of TFI and PDFI. Concentration: TFI (curve a), 2×10^{-6} mol/L; PDFI (curve b), 2×10^{-6} mol/L

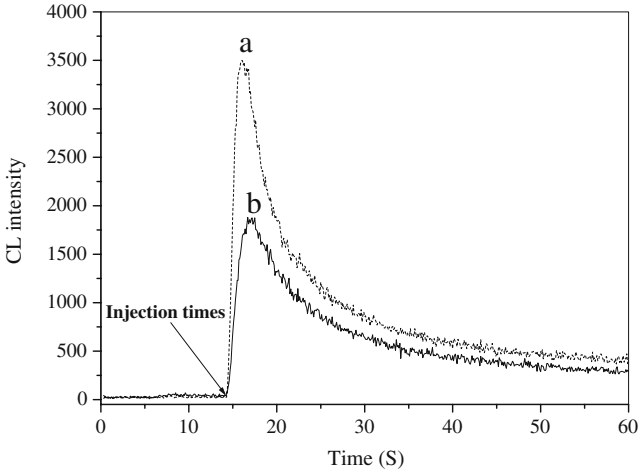

Fig. 5 CL kinetic curves of TFI and PDFI. Concentration: **a** TFI, 0.1 mmol/L; H_2SO_4, 0.5 mol/L; $KMnO_4$, 1 mmol/L. **b** PDFI, 0.1 mmol/L; H_2SO_4, 0.5 mol/L; $KMnO_4$, 1 mmol/L

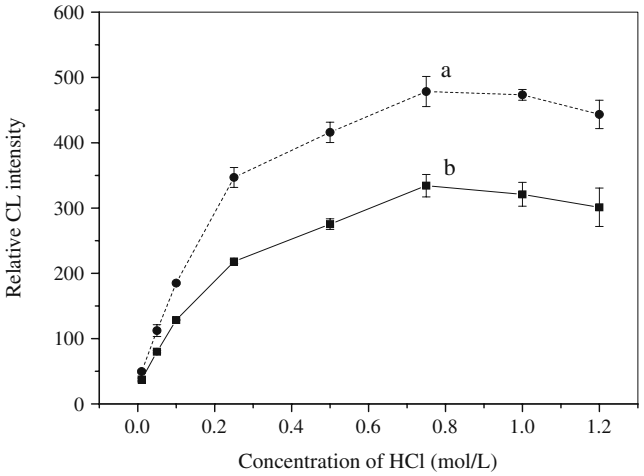

Fig. 7 Influence of HCl concentration on the CL intensity. Concentration: **a** TFI, 0.1 mmol/L; $KMnO_4$, 1 mmol/L. **b** PDFI, 0.1 mmol/L; $KMnO_4$, 1 mmol/L. The error bars denote the standard deviation of the values with the three same determinations

the mixture was cooled to room temperature, diluted with 100 mL of water, and then neutralized with a 20% NaOH aqueous solution to pH 9. The mixture was extracted with ethyl acetate, and the solvent was removed. The ethyl acetate was evaporated by rotary evaporation. The crude product was further purified by column chromatography using a mixture of petroleum ether and ethyl acetate (3:1) as eluents. Then TFI was recrystallized from methanol. Yellow single crystals were obtained by slow evaporation of the solvent at ambient temperature.

PDFI was synthesized according to the literature [31]. A mixture of 0.82 g furil (4.32 mmol) and 4.05 g ammonium acetate (52.60 mmol) in 20 mL acetic acid was stirred to form homogeneous solution at room temperature. Then, benzaldehyde (4.75 mmol) was added to the mixture. The reaction mixture was heated and refluxed. After furil was completely reacted, the reaction mixture was cooled to room temperature, poured into 100 mL of water, and then neutralized with an aqueous solution of 20% NaOH to pH 9. The mixture was extracted with ethyl acetate. The organic layer was separated, washed with water, and dried over $MgSO_4$. The ethyl acetate was evaporated in vacuo, and the residue was purified by recrystallization after column chromatography on Chemapol silica gel (eluent, petroleum ether/EtOAc=3/1) to obtain PDFI.

Characterization of TFI and PDFI

The TFI and PDFI were characterized by melting point, IR, MS and NMR. The results obtained by elemental analysis

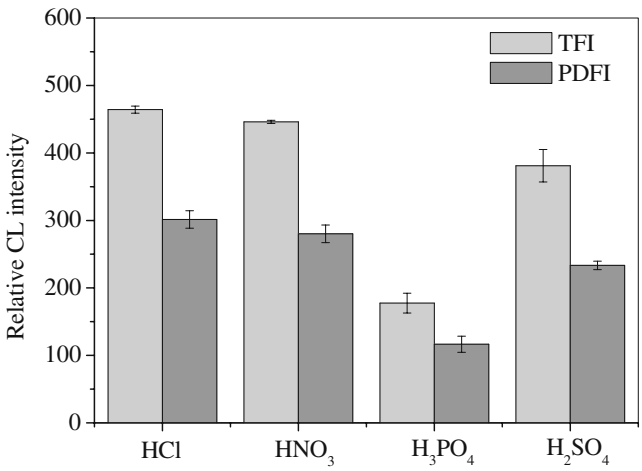

Fig. 6 The effect of acids on CL intensity. Concentration: TFI, 0.1 mmol/L; PDFI, 0.1 mmol/L; acids, 0.5 mol/L; $KMnO_4$, 1 mmol/L. The error bars denote the standard deviation of the values with the three same determinations

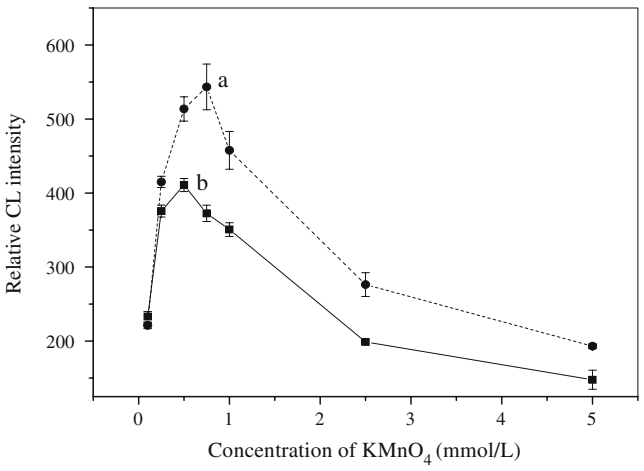

Fig. 8 Influence of $KMnO_4$ concentration on the CL intensity. Concentration: **a** TFI, 0.1 mmol/L; HCl, 0.75 mol/L. **b** PDFI, 0.1 mmol/L; HCl, 0.75 mol/L. The error bars denote the standard deviation of the values with the three same determinations

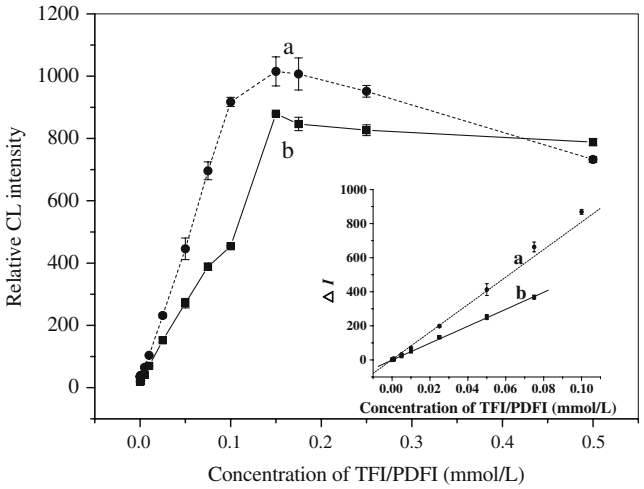

Fig. 9 Influence of TFI/PDFI concentration on the CL intensity. The inset displays the linear relationship between ΔI and the concentration of TFI/PDFI. **a** TFI-$KMnO_4$ system and **b** PDFI-$KMnO_4$ system. Concentration: **a** HCl, 0.75 mol/L; $KMnO_4$, 0.75 mmol/L. **b** HCl, 0.75 mol/L; $KMnO_4$, 0.5 mmol/L. The error bars denote the standard deviation of the values with the three same determinations

were in conformity with the theoretical results. The results are described as follows.

2,4,5-Tri(2-Furyl)-1H-Imidazole (TFI)

M.p. 196–197°C. IR (KBr) ν (cm^{-1}): 3417, 3114, 2926, 1627, 1538, 1477, 1430, 1380, 1201, 1016, 887, 748. ^1H NMR (500 MHz, $CDCl_3$), δ (ppm): 10.48 (s, 1H), 7.42 (s, 2H), 7.36 (s, 1H), 6.92 (d, J=3.3 Hz, 3H), 6.46 (dd, J=3.0, 1.7 Hz, 2H), 6.41 (dd, J=3.1, 1.6 Hz, 1H). MS (m/z): $(M + H)^+$ 267.3 (Calcd 266.25). Calcd for $C_{15}H_{10}N_2O_3$: C, 67.65; H, 3.79; N, 10.53. The elemental analysis gave the molecular formula $C_{15}H_{10}N_2O_3$ (Found: C, 67.53; H, 3.71; N, 10.45).

2-Phenyl-4,5-di(2-Furyl)-1H-Imidazole (PDFI)

M.p.197–198°C. IR (KBr) ν (cm^{-1}): 3118, 3054, 1599, 1551, 1481, 1404, 1233, 1090, 886, 732, 590. ^1H NMR (300 MHz, $CDCl_3$), δ (ppm): 7.92 (dd, J=8.2, 1.5 Hz, 2H), 7.57–7.33 (m, 5H), 6.99 (d, J=3.3 Hz, 2H), 6.53 (dd, J= 3.4, 1.8 Hz, 2H). MS (m/z): $(M + H)^+$ 277.9 (Calcd 276.29). Calcd for $C_{17}H_{12}N_2O_2$: C, 73.80; H, 4.38; N, 10.14. The elemental analysis gave the molecular formula $C_{17}H_{12}N_2O_2$ (Found: C, 73.55; H, 4.34; N, 9.95).

Apparatus

The CL analysis was conducted on a laboratory-built steady injection CL system. The schematic diagram of the system is shown in Fig. 3. The steady injection Analysis Processor FIA-3100 (Beijing Wantuo Instruments Co. Ltd.) consists of two peristaltic pumps, a sixteen-hole eight-way valve and a digital-system to control the time and pump pressure. PTFE tube (0.8 mm i.d.) was used as connection material in the steady system. The CL emission was detected by an ultra-weak luminescence analyzer (type BPCL manufactured at the Institute of Biophysics, Chinese Academy of Sciences, Beijing, China). The acquisition and treatment of data were performed with BPCL software running under Windows XP.

PL spectra were recorded on a RF-5301 spectrofluorimeter (Shimadzu, Japan). The absorption spectra were recorded on an Australian GBC Cintra 10e UV–vis Spectrometer within the wavelength range from 200 to 800 nm.

Procedure

Experimental results were obtained using the following operation parameters: pump rate, 60 rpm/min; sample loop volume, 300 μL; sampling time, 12 s; sample injection time, 20 s; the PMT negative voltage, −900 V; the integral time of the CL signal, 60 s. 200 μL of TFI/PDFI solution (or solution containing TFI/PDFI and albumin) was first added into the sample cell (colorless glass tube 1 cm i.d.), and then $KMnO_4$ and HCl solution were synchronously injected into the sample cell using the steady injection system.

In sequence 1 (Fig. 3a), pumps P_1 and P_2 were activated, and valve V was in the loading position. The pump P_1 was used to deliver $KMnO_4$ solution into the sample $loop_1$ (SL_1) and the pump P_2 was used to introduce HCl solution into the sample $loop_2$ (SL_2). In sequence 2 (Fig. 3b), pumps P_1 and P_2 were activated, and valve V was in the injection position. The pumps P_1 and P_2 were used to deliver the air current. The $KMnO_4$ solution and HCl solution were simultaneously pumped at the same rate separately into chemifold R where they were mixed. The mixed solution was carried into sample cell S and mixed with TFI/PDFI (or solution containing TFI/PDFI and albumin) in the sample cell S. CL signal was measured

Table 1 Linear calibration equation for TFI/PDFI

System	Calibration curve (C, mmol/L)	Linear range (mol/L)	R	Detection limit (mol/L)	RSD (%)
TFI-$KMnO_4$	ΔI=8077C + 1.513	1.0×10^{-8}–1.0×10^{-4}	0.9935	3.6×10^{-9}	2.0
PDFI-$KMnO_4$	ΔI=4976C–1.295	5.0×10^{-8}–7.5×10^{-5}	0.9973	3.4×10^{-8}	3.0

The RSD was estimated at 5.0×10^{-6} mol/L for TFI/PDFI (n=11)

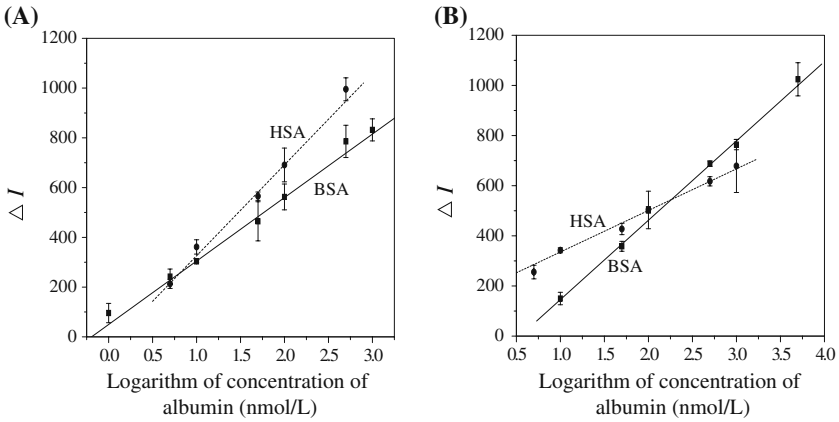

Fig. 10 Calibration curves for the determination of HSA and BSA. **A** TFI-$KMnO_4$ system and **B** PDFI-$KMnO_4$ system

and recorded. After determination, the mixed solution in the sample cell S was emptied. The sample cell S was washed and dried. All experiments were performed in triplicate.

The concentration of analyte was quantified by measuring the change of CL intensity. $\Delta I = I_s - I_0$, where I_0 and I_s are CL signals in the absence and presence of analyte, respectively.

Preparation of Sample

Human serum samples obtained from the Qianwei Hospital of Jilin University were analysed. 300 μL of sample and an equal volume of normal saline (NS) were mixed, and added into a 2 mL centrifuge tube. 600 μL of saturated ammonium sulfate solution was added dropwise into the centrifuge tube when the solution was stirred continuously. The solution was at rest for 1 h, and then centrifugalized for 30 mins at 4000 rpm/min. The upper solution was added into a flask and the lower sediment was dissolved in 600 μL of NS. 300 μL of saturated ammonium sulfate solution was added dropwise into resulted solution from the sediment when the solution was stirred continuously. The solution was centrifugalized for 30 mins at 4000 rpm/min. Then the upper solution obtained was also added into the flask. To purify the solution, the free ions were removed via dialysis for 24 h in water (4°C)

Results and Discussion

Absorption Spectra, PL Spectra and CL Kinetic Curves of TFI and PDFI

Figure 4 shows the absorption spectra (Fig. 4A) and PL spectra (Fig. 4B) of TFI and PDFI. It can be seen from Fig. 4A that the first excitonic absorption peaks of the TFI and PDFI appear at 316 and 314 nm, respectively. The PL spectra show that the excitation peaks of TFI and PDFI are at around 319 and 317 nm, respectively, corresponding with the emission peaks of 422 and 435 nm. The CL reaction between TFI/PDFI and $KMnO_4$ was further investigated in acid medium. The $KMnO_4$ can, in the available concentration range, directly oxidize TFI and PDFI to generate strong CL emission. The dynamic CL intensity-time profiles of the TFI-$KMnO_4$ and PDFI-$KMnO_4$ systems are shown in Fig. 5.

Effect of Acids

The effects of kinds of acids, including HCl, HNO_3, H_3PO_4 and H_2SO_4, on the TFI/PDFI-$KMnO_4$ CL system were examined. The results are shown in Fig. 6. It can be seen that the highest emission was observed in HCl medium. Hence, the HCl solution was chosen as the reaction medium.

The effect of the concentration of HCl on the CL intensity of TFI/PDFI-$KMnO_4$ system was examined in the

Table 2 Standard curves for albumins

System	Albumin	Calibration curve (C, nmol/L)	r	Linear range (mol/L)	Detection limit (mol/L)	RSD (%)
TFI-$KMnO_4$	BSA	ΔI=259.4lgC + 44.94	0.9952	1.0×10^{-9}–1.0×10^{-6}	3.5×10^{-10}	2.5
	HSA	ΔI=365.8lgC–39.89	0.9952	5.0×10^{-9}–5.0×10^{-7}	1.2×10^{-9}	1.6
PDFI-$KMnO_4$	BSA	ΔI=316.5lgC–170.9	0.9990	1.0×10^{-8}–5.0×10^{-6}	4.5×10^{-9}	3.1
	HSA	ΔI=165.7lgC + 169.8	0.9945	5.0×10^{-9}–1.0×10^{-6}	1.7×10^{-9}	1.8

The RSD was estimated under 1.0×10^{-7} mol/L for albumin (n=11)

Table 3 Tolerance of foreign substances

Substance	Concentration (μmol/L)	TFI-$KMnO_4$ system change of ΔI (%)	Concentration (μmol/L)	PDFI-$KMnO_4$ system change of ΔI (%)
Na^+, Cl^-	500	−0.3	500	−3.1
K^+, Cl^-	500	2.7	500	−0.8
Ca^{2+}, Cl^-	500	−1.8	500	−4.4
Mg^{2+}, Cl^-	500	0.6	500	0.4
Ba^{2+}, Cl^-	500	−2.1	500	−0.5
Al^{3+}, SO_4^{2-}	500	4.9	500	−2.5
Zn^{2+}, Cl^-	500	−3.2	250	3.0
Cu^{2+}, SO_4^{2-}	500	0.9	100	1.3
Mn^{2+}, SO_4^{2-}	25	−1.4	25	−4.5
Fe^{2+}, Cl^-	50	4.5	10	−1.2
Carbamide	500	2.7	500	1.4
Glucose	500	0.6	500	−4.3
L-Tryptophan	500	−3.7	500	−4.6
L-Tyrosine	25	4.9	10	4.6
DL-β-Phenylalanine	500	3.2	250	−3.8
L-Asparagine	250	−0.4	500	3.9

Concentration of HSA is 1.0×10^{-7} mol/L

range of 0.01–1.2 mol/L, and the results are shown in Fig. 7. The CL intensity increases when the HCl concentration increases from 0.01 to 0.75 mol/L, and the intensity starts to decrease when the concentration is higher than 0.75 mol/L. Therefore, the optimum HCl concentration was chosen to be 0.75 mol/L for TFI/PDFI-$KMnO_4$ system.

Effect of the Concentration of $KMnO_4$

The effect of the $KMnO_4$ concentration on the CL intensity was studied, and the plot of CL intensity versus $KMnO_4$ concentration is shown in Fig. 8. From Fig. 8, it can be seen that the CL intensity increases with the increase of the concentration of $KMnO_4$. The CL intensity reaches a maximum when the concentrations of $KMnO_4$ are 0.75 mmol/L and 0.5 mmol/L for TFI-$KMnO_4$ and PDFI-$KMnO_4$ systems, respectively. When the concentrations of $KMnO_4$ are higher than 0.75 mmol/L and 0.5 mmol/L for TFI-$KMnO_4$ and PDFI-$KMnO_4$ systems, respectively, the CL intensity of the TFI/PDFI-$KMnO_4$ system decreases with the increase of $KMnO_4$ concentration. So 0.75 mmol/L and 0.5 mmol/L $KMnO_4$ were chosen for further research, respectively.

Effect of the Concentration of TFI/PDFI

The effect of TFI/PDFI concentration on the CL intensity of the studied system was tested. From Fig. 9, it can be seen that the concentration of the TFI/PDFI has great influence on the CL intensity. With the increase of concentration of TFI/PDFI, the CL intensity increases when the concentration of TFI/PDFI is lower than 0.15 mmol/L, and the intensity decreases when the concentration of TFI/PDFI is higher than 0.15 mmol/L. Therefore, the optimum concentration of TFI/PDFI was chosen to be 0.15 mmol/L.

There is a good linear relationship between the enhanced CL intensity and the concentration of TFI/PDFI in the range of low concentration (Fig. 9 inset). The regression equations of calibration curves, detection limits and relative standard deviations (RSDs) are summarized in Table 1. The results demonstrate that the proposed CL system may be used to detect TFI/PDFI.

Table 4 Determination of HSA in human serum samples

Sample	Bomocresol green (g/L)	TFI-$KMnO_4$ system (g/L) (n=5)	Relative error (%)	PDFI-$KMnO_4$ system (g/L) (n=5)	Relative error (%)
1	47	46±1.5	−2.1	45±0.6	−4.3
2	50	51±2.1	2.0	50±1.4	0.0
3	46	45±1.1	−2.2	45±1.8	−2.2
4	48	50±1.0	4.2	46±2.1	−4.2
5	50	52±1.9	4.0	51±1.8	2.0
6	52	49±1.9	−5.8	50±1.5	−3.8

Determination of Albumin

The influences of albumins BSA and HSA on the CL intensity of the TFI/PDFI-$KMnO_4$ system were examined. It was found that the addition of albumin into the system could induce enhancement of CL signal. Based on the enhancing of CL for TFI/PDFI-$KMnO_4$ system by albumin, a sensitive CL enhancing method has been developed for the determination of albumin. The calibration graphs were constructed under the optimal conditions, and the results are shown in Fig. 10. It can be seen from Fig. 10 that the CL response of the TFI/PDFI-$KMnO_4$ system increases in the presence of the two kinds of albumins BSA and HSA. The experimental parameters are given in Table 2. It demonstrates that there are satisfactory linear relationships, wide linear ranges and high sensitivity.

Selectivity

The interference of various foreign substances was tested when the concentration of HSA was 1.0×10^{-7} mol/L. The results are listed in Table 3. It can be seen from Table 3 that most of the coexisting substances do not interfere with the detection of HSA. The proposed method is quite selective for determination of HSA. This fact was further attested by applying the present method to the determination of HSA in some samples.

Analytical Application

The method finds an excellent application for the determination of HSA in the human serum samples. The results are shown in Table 4. The human serum samples, which were diluted 10000-fold, were analyzed. The results obtained were found to be in agreement with the commonly used bromocresol green (BCG) method.

Conclusion

This work is concerned with the CL of 2-substituted-4,5-di (2-furyl)-*1H*-imidazoles TFI and PDFI in solution. The strong CL signals were observed when TFI/PDFI was mixed with $KMnO_4$ in acidic solution. The effects of experimental conditions were investigated. Meanwhile the increase of CL intensity of the TFI/PDFI-$KMnO_4$ system is proportional to the concentration of TFI/PDFI in the range of low concentration. The addition of albumin into the system could induce enhancement of CL signal. Based on this study, it was found that the TFI/PDFI-$KMnO_4$ CL system could be successfully applied to the simultaneous determination of TFI/PDFI and albumin. To evaluate practical application for the proposed method, human serum samples were analyzed and the obtained results were satisfactory. By comparison with some existing methods [32–34], the proposed method has advantages of high selectivity and sensitivity, instrumental simplicity, low cost and wide linear response range for determination of albumin. This may intrigue researchers into gaining a new interest in investigating the CL property of heterocyclic imidazole derivatives.

References

1. Santos J, Mintz EA, Zehnder O, Bosshard C, Bua XR, Günterb P (2001) New class of imidazoles incorporated with thiophenevinyl conjugation pathway for robust nonlinear optical chromophores. Tetrahedron Lett 42:805–808
2. Fridman N, Speiser S, Kaftory M (2006) Structures and chromogenic properties of bisimidazole derivatives. Cryst Growth Des 6:1653–1662
3. Fridman N, Speiser S, Kaftory M (2006) Chromotropic behavior of lophine nitro-derivatives. Cryst Growth Des 6:2281–2288
4. Nashima K (2003) Lophine derivatives as versatile analytical tools. Biomed Chromatogr 17:83–95
5. Uçucu Ü, Karaburun NG, Işikdağ I (2001) Synthesis and analgesic activity of some 1-benzyl-2-substituted-4, 5-diphenyl-1H-imidazole derivatives. IL Farmaco 56:285–290
6. Testa AC (2000) Laser flash photolysis study of triphenylimidazole. Spectrochim Acta Part A 56:901–904
7. Chou P, McMorrow D, Aartsma TJ, Kasha M (1984) The proton-transfer laser. Galn spectrum and ampllficatlon of spontaneous emission of 3-hydroxyflavone. J Phys Chem 88:4596–4599
8. Kimura M, Lu GH, Iga H, Tsunenaga M, Zhang ZQ, Hu ZZ (2007) The stereoselective thermal rearrangement of chiral lophine peroxides. Tetrahedron Lett 48:3109–3113
9. Fridman N, Kaftory M, Speiser S (2007) Structures and photophysics of lophine and double lophine derivatives. Sens Actuators B 126:107–115
10. Nakashima K, Yamasaki H, Kuroda N, Akiyama S (1995) Evaluation of lophine derivatives as chemiluminogens by a flow-injection method. Anal Chim Acta 303:103–107
11. Fridman N, Kaftory M, Eichen Y, Speiser S (2009) Crystal structures and solution spectroscopy of lophine derivatives. J Mol Struct 917:101–109
12. Nakashima K, Fukuzaki Y, Nomura R, Shimoda R, Nakamura Y, Kuroda N, Akiyama S, Irgum K (1998) Fluorescence and chemiluminescence properties of newly developed lophine analogues. Dyes Pigm 38:127–136
13. Siddiqui SA, Narkhede UC, Palimkar SS, Daniel T, Lahoti RJ, Srinivasan KV (2005) Room temperature ionic liquid promoted improved and rapid synthesis of 2, 4, 5-triaryl imidazoles from aryl aldehydes and 1, 2-diketones or a-hydroxyketone. Tetrahedron 61:3539–3546
14. Marquette CA, Blum LJ (2006) Applications of the luminol chemiluminescent reaction in analytical chemistry. Anal Bioanal Chem 385:546–554
15. Tsukagoshi K, Nakahama K, Nakajima R (2004) Direct detection of biomolecules in a capillary electrophoresis-chemiluminescence detection system. Anal Chem 76:4410–4415
16. Gámiz-Gracia L, García-Campaña AM, Soto-Chinchilla JJ, Huertas-Pérez JF, González-Casado A (2005) Analysis of pesticides by chemiluminescence detection in the liquid phase. Trends Anal Chem 24:927–942
17. Fletcher KA, Fakayode SO, Lowry M, Tucker SA, Neal SL, Kimaru IW, McCarroll ME, Patonay G, Oldham PB, Rusin O,

Strongin RM, Warner IM (2006) Molecular fluorescence, phosphorescence, and chemiluminescence spectrometry. Anal Chem 78:4047–4068
18. Nakashima K, Yamasaki H, Shimoda R, Kuroda N, Akiyama S, Baeyens WRG (1997) Flow-injection analysis of cobalt (II) utilizing enhanced lophine chemiluminescence with hydroxylammonium chloride. Biomed Chromatogr 11:63–64
19. Marho DF, Ingle JD Jr (1981) Determination of chromium (VI) in water by lophine chemiluminescence. Anal Chem 53:294–298
20. MacDonald A, Chan KW, Nieman TA (1979) Lophine chemiluminescence for metal ion determinations. Anal Chem 51:2077–2082
21. Marho DF, Ingle JD Jr (1981) Ion exchange separation of cobalt from alkaline earth and selected transition metals with lophine chemiluminescence detection. Anal Chem 53:292–294
22. Benjamin JH, Neil WB (2001) Analytical applications of acidic potassium permanganate as a chemiluminescence reagent. Anal Chem Acta 445:1–19
23. Chen H, Lu C, Li RB, Guo GS, Lin JM (2010) Chemiluminescence behavior of sodium hydrogen carbonate in the potassium permanganate-hydrogen peroxide reaction. Sci China Chem 53:1784–1792
24. Galera MM, García MDG, Valverde RS (2008) Determination of photoirradiated high polar benzoylureas in tomato by HPLC with luminol chemiluminescence detection. Talanta 76:815–823
25. Adcock JL, Francis PS, Barnet NW (2007) Acidic potassium permanganate as a chemiluminescence reagent—a review. Anal Chem Acta 601:36–67
26. Bree AG, Neil WB, Richard B (2005) Detection of pyrrolizidine alkaloids using flow analysis with both acidic potassium permanganate and tris(2, 2′-bipyridyl)ruthenium (II) chemiluminescence. Anal Chem Acta 541:119–124
27. Han HY, He ZK, Zeng YE (2006) Chemiluminescence method for the determination of glutathione in human serum using the Ru $(phen)_3^{2+}$–$KMnO_4$ system. Microchim Acta 155:431–434
28. Slezak T, Terry JM, Francis PS, Hindson CM, Olson DC, Wolcott DK, Barnett NW (2010) Autocatalytic nature of permanganate oxidations exploited for highly sensitive chemiluminescence detection. Anal Chem 82:2580–2584
29. Hindson CM, Francis PS, Hanson GR, Adcock JL, Barnett NW (2010) Mechanism of permanganate chemiluminescence. Anal Chem 82:4174–4180
30. Wang SJ, Gu Q, Su Q, Chen XD, Zhang YM (2009) 2,4,5-Tri-2-furyl-1H-imidazole. Acta Crystallogr Sect E Struct Rep 65: O3194-U1481
31. Wang J, Mason R, VanDerveer D, Feng K, Bu XR (2003) Convenient preparation of a novel class of imidazo[1, 5-a] pyridines: decisive role by ammonium acetate in chemoselectivity. J Org Chem 68:5415–5418
32. Deftereos NT, Grekas N, Calokerinos AC (2000) Flow injection chemiluminometric determination of albumin. Anal Chim Acta 403:137–143
33. Jiang CQ, Luo L (2004) Spectrofluorimetric determination of human serum albumin using a doxycycline–europium probe. Anal Chim Acta 506:171–175
34. Dong LJ, Li Y, Zhang YH, Chen XG, Hu ZD (2007) A flow injection sampling resonance light scattering system for total protein determination in human serum. Spectrochim Acta Part A 66:1317–1322